Mesozoic 001 (3): 379–388
https://www.mapress.com/mz/

Article

ISSN 3021-1859 (print edition)
MESOZOIC
ISSN 3021-1867 (online edition)

https://doi.org/10.11646/mesozoic.1.3.17
http://zoobank.org/urn:lsid:zoobank.org:pub:4CF90FD5-0DBC-4DC0-A6B3-05F0E2E4F2F5

Palaeoenvironmental analysis of the Langshan Formation in the Xiongba area

YI-WEI XU[1,*], WEN LAI[2] & XIU-MIAN HU[3]

[1]*State Key Laboratory of Palaeobiology and Stratigraphy, Nanjing Institute of Geology and Palaeontology, Chinese Academy of Sciences, Nanjing 210008, China*
[2]*School of Geography and Environmental Engineering, Gannan Normal University, Ganzhou 341000, China*
[3]*State Key Laboratory of Mineral Deposits Research, School of Earth Sciences and Engineering, Nanjing University, Nanjing 210023, China*

kongjuzixing@126.com; https://orcid.org/0000-0002-3387-7453
nju_laiwen@163.com; https://orcid.org/0009-0005-6948-4730
huxm@nju.edu.cn; https://orcid.org/0000-0002-5401-8682
**Corresponding author*

Abstract

The mid-Cretaceous Langshan Formation is a massive limestone unit, outcropping typically in the northern Lhasa block. A Xiongba section, measured near the type section of the Langshan Formation, is here described. The succession consists of orbitolinids limestone, where eight microfacies have been recognized. The lower part of the Langshan Formation consists of discoidal orbitolinids with other heterotrophic associations, including echinoderms, sponge spicules, and bivalves. In contrast, the upper part of the Langshan Formation features conical orbitolinids with an abundance of green algae and small benthic foraminifers. We interpret the morphological changes in orbitolinids as being influenced by bathymetry. Consequently, the microfacies variations in the Langshan Formation in the Xiongba section represent a shallowing upward sequence.

Keywords: Lhasa block, Langshan Formation, carbonate microfacies, mid-Cretaceous, palaeogeography

Introduction

The Lhasa block is the last microcontinent to accrete onto the southern margin of the Asian plate before the collision of the Indian and Asian continental margins (Yin & Harrison, 2000; Kapp *et al*., 2007; Hu *et al*., 2022). Although the precise timing of the collision between the Qiangtang and Lhasa blocks remains debated, it is generally accepted that this progress occurred before the Early Cretaceous (Dewey *et al*., 1988; Fan *et al*., 2014; Zhu *et al*., 2016; Ma *et al*., 2017; Li *et al*., 2019). Thick mid-Cretaceous carbonate rocks, referred to as the Langshan Formation, were accumulated in the central Tibet following the collision and represent the latest marine unit of the Lhasa block (Pan *et al*., 2004; Leier *et al*., 2007; Xu *et al*., 2020, 2022). Understanding the palaeogeographic evolution of this unit is crucial, as it enhances our comprehension of the basin evolution of the Lhasa block and the tectonic framework of the Tibet prior to the India-Asia collision.

Several published works have analyzed the sedimentology and palaeogeography of the Langshan Formation (Leeder *et al*., 1988; Zhang *et al*., 2004; Leier *et al*., 2007; Sun *et al*., 2017; Lai *et al*., 2019a; Xu *et al*., 2022). While detailed studies focus on the palaeoenvironmental changes within long sections (over 1 kilometer) well exposed along the southern and northern edge of the Langshan Formation outcrop belt, the sedimentological analysis of the Langshan Formation in central area has relied on only poorly preserved sections with a thickness of less than 100 meters (Xu *et al*., 2022). This lack of investigation in the central region hinders our full understanding of the mid-Cretaceous palaeogeographic evolution of the northern Lhasa block.

The mid-Cretaceous strata exposed near the Duba village, which is located close to the type section of the Langshan Formation, offer an opportunity to advance research on the palaeoenvironmental analysis of the Langshan Formation in the central area. In this study, we describe the Xiongba section measured at Duba, near the Seling Co Lake, where the succession is well exposed and consists of orbitolinids-rich limestone. This study presents new data on the sedimentology of the Langshan Formation and provides insights into the palaeogeographic evolution of the Lhasa block during the mid-Cretaceous.

Submitted: 19 Sept. 2024; accepted by D.-Y. Huang: 26 Sept. 2024; published: 30 Sept. 2024

Geological setting

The Lhasa block is divided into the southern Lhasa and northern Lhasa blocks separated by the Luobadui–Milashan Fault (Fig. 1A) (Pan *et al*., 2004; Kapp & DeCelles, 2019). Thick Cretaceous sedimentary sequences were accumulated in the northern Lhasa block, which include the Duoni, Langshan, and Jingzhushan formations (Pan *et al*., 2004; Sun *et al*., 2015; Lai *et al*., 2019a, b; Fig. 1B).

The Duoni Formation consists of siliciclastics sourced from the Zenong volcanic rocks or the Bangong suture and southern Qiangtang block (Leier *et al*., 2007; Zhang *et al*., 2011; Sun *et al*., 2017; Lai *et al*., 2019a). The depositional age of this unit is constrained between 123–110 Ma based on detrital-zircon chronostratigraphy and the age of intercalated volcanic rocks (Leier *et al*., 2007; Sun *et al*., 2017; Lai *et al*., 2019a; Zhu *et al*., 2022). The depositional sequences of the Duoni Formation exhibit a typically shallowing upward trend, with depositional environments transitioning from deep shelf to fluvial floodplain (Leier *et al*., 2007; Sun *et al*., 2017; Lai *et al*., 2019a).

The Langshan Formation conformably overlies the Duoni Formation has a depositional age ranging from early Aptian to middle Cenomanian based on biostratigraphy (Rao *et al*., 2015; BouDagher-Fadel *et al*., 2017; Xu *et al*., 2020, 2022). The lithology of Langshan Formation varies across the northern Lhasa block, which is represented by pure limestone in the central area, by limestone interbedded with siliciclastic rocks in the southern area, and by limestone interbedded with marls in the northern area (Xu *et al*., 2022). The depositional environments of the Langshan Formation are generally of shallow marine, but they vary from intertidal to open marine settings depending on geographic locations (Leeder *et al*., 1988; Leier *et al*., 2007; Xu *et al*., 2020, 2022). The depositional geometry of the Langshan Formation transitioned from a ramp to a rimmed platform during the Albian and reverted to a ramp during the early Cenomanian (Xu *et al*., 2022).

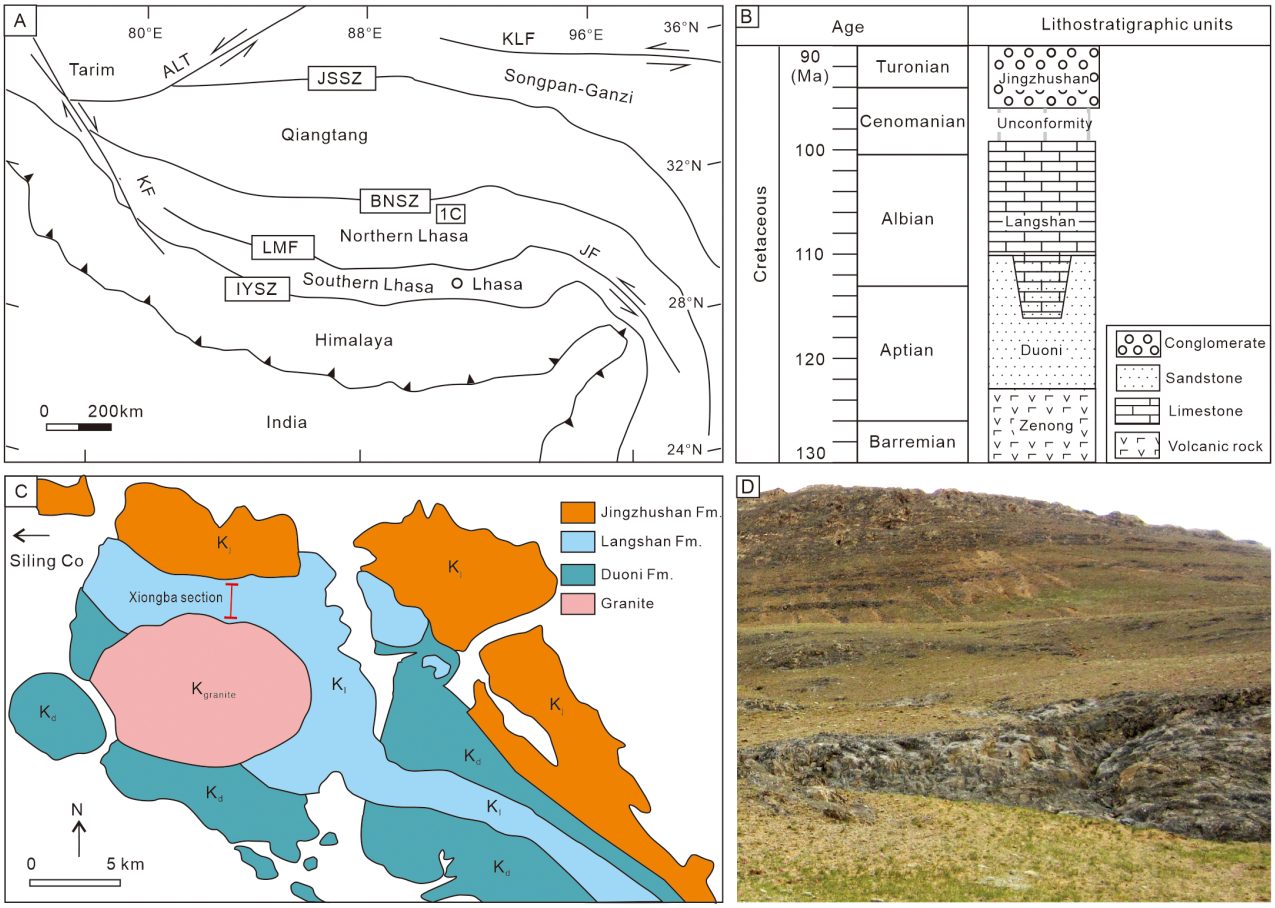

FIGURE 1. Geological sketch map showing the tectonic units of the Tibet, along with sampling locations. **A**, Simplified tectonic map of the Himalaya and Tibet showing major tectonic domains and suture zones (Pan *et al*., 2004). **B**, Cretaceous strata in the Northern Lhasa terrane (Xu *et al*., 2022). **C**, Simplified geological map of the Duba village, showing the studied sections. **D**, The stratigraphic column of the sampling section. BNSZ, Bangong–Nujiang suture zone; IYZS, Indus–Yarlung–Zangbo suture; JSSZ, Jinshajiang suture zone; LMF, Luobadui–Milashan fault; JF, Jiali fault; KLF, Kunlun fault; KF, Karakoram fault; ALT, Altyn Tagh fault.

The Jingzhushan Formation, exposed to the north of the Langshan Formation outcrop belt, consists of fluvial to alluvial conglomerates, with minor red sandstone and siltstone primarily derived from the erosion of the Langshan Formation and the Zenong Group (Sun *et al*., 2015; Lai *et al*., 2019b). The depositional age of the Jingzhushan Formation is constrained to the late Cenomanian-Turonian, based on the age of intercalated tuffs (Sun *et al*., 2015; Lai *et al*., 2019b).

The studied area is located in the Baingoin Basin (Fig. 1C), where Lower Cretaceous strata, including the Duoni, Langshan, and Jingzhushan formations, are widespread and well exposed. Recently published zircon U-Pb ages near the Duba village indicate that the Duoni Formation was deposited during 122–110 Ma, while the Jingzhushan Formation was deposited during 100–90 Ma (Lai *et al*., 2019a, b).

Material and methods

The Xiongba section is exposed to the southeast of the Seling Co lake (31°30′54.68″ N; 89°29′59.04″ E) (Fig. 1D). This study focuses on the Langshan Formation with a thickness of 293 meters, where samples were collected with an average spacing of 2–3 m. A total of 76 thin sections were used for microfacies analysis based on field observations, grain components, textures, and fossil assemblages. Carbonate rocks were classified based on Dunham (1962).

Results

Based on field observations, textural features, and fossil assemblages, eight microfacies (MF1 to MF8) were recognized in the Xiongba section, representing three sedimentary facies.

MF1 Bioclast- discoidal orbitolinid wackestone

Description: This microfacies is featured by discoidal orbitolinids (3–10 mm in diameter, 10%–30%) set in the micritic matrix with echinoderms and sponge spicules (5%–20%) (Fig. 2A). Bivalve debris are minor, while green algae and ostracods are largely absent. Stylolites are commonly found within the matrix.

Interpretation: The morphology of orbitolinids is generally related to water depth, with increased width-height ratios (*i.e*., discoidal orbitolinids) associated with deeper environments (Banner & Simmons, 1994; Vilas *et al*., 1995). The occurrence of sponge spicules and echinoderms implies a heterotrophic assemblage that is common in relatively deep subtidal conditions (Halfar *et al*., 2004).

MF2 Discoidal orbitolinid packstone

Description: In the MF2, orbitolinids represent 70–85% of the rock components and are associated with echinoderms, bivalves, sponge spicules, and other bioclasts (Fig. 2B). Most orbitolinids are flat and well preserved with a diameter of 2–6 mm, although some are conical and smaller in size (1–2 mm) compared to the flattened species. Additionally, some debris from orbitolinids can be observed. Stylolites are commonly found among the orbitolinids.

Interpretation: The variation in size among orbitolinids and their broken debris suggest hydraulic sorting during transportation, with discoidal orbitolinids being more easily suspended than conical species. The carbonate mud matrix, containing smaller bioclasts, indicates the deposition in low-energy conditions. The interbedding of MF2 with MF1 represents a background of relatively deep subtidal environments. The grain-supported texture, along with the broken orbitolinids, suggests deposition during periods of higher energy conditions, such as storms.

MF3 Bivalve wackestone

Description: This microfacies is featured by sparse bivalve debris (15%) set in the micritic matrix. Echinoderms and sponge spicules (5%) are minor (Fig. 2C). MF3 is rare and interbedded with MF2 in the Xiongba section.

Interpretation: The dominance of micritic matrix suggests a low-energy environment, while its association with MF2 indicates a relatively deep subtidal setting.

MF4 Sponge spicule wackestone

Description: Abundant sponge spicules (15%–20%) are in the micritic matrix (Fig. 2D). These spicules are recrystallized to clean calcite spar. Other bioclasts, including conical orbitolinids, small benthic foraminifers, echinoderms, and bivalves, are present with minor amounts (5–10%).

Interpretation: Although carbonates rich in spicules are traditionally interpretated as deposition in deep basins (Wilson, 1975), sponges can also thrive in much shallower marine environments (James & Jones, 2015). The co-occurrence of conical orbitolinids and small benthic foraminifers further implies a shallow subtidal condition (Davies *et al*., 2002).

MF5 Spicule-conical orbitolinid wackestone

Description: Conical orbitolinids with a diameter of 1–1.5 mm (20%–30%) set in micritic matrix with abundant sponge spicules (5%–10%) (Fig. 2E). Echinoderms are minor (3%–8%). Green algae and ostracods are rare.

Interpretation: Conical orbitolinids exhibit low width–height ratios, which are common associated with shallow subtidal environments (Banner & Simmons, 1994; Vilas *et al*., 1995).

MF6 Small benthic foraminifer-conical orbitolinid wackestone

Description: Thick-bedded limestones in the upper part of the Xiongba section mainly consists of conical orbitolinids (10%–25%), various kinds of small benthic foraminifers (including miliolids and textulariids, 3%–5%), and peloids (15%–20%) (Fig. 2F). Echinoderms, sponge spicules, and green algae are sparse distributed in the micritic matrix (3%).

Interpretation: The diverse small benthic foraminifers representing a very shallow environments (Davies *et al*., 2002). The assemblage of biota is typical of Cretaceous shallow-water marine environment (Davies *et al*., 2002). The high species diversity indicates an open shallow subtidal environment. Microfacies MF6, interbedded with MF8, suggests a very shallow subtidal setting.

MF7 Orbitolinids-green algae wackestone to packstone

Description: Strata with orbitolinids (15%–20%) and green algae (5–10%) set in micritic matrix occur at the middle part of the Xiongba section (Fig. 2G). The shape of orbitolinids varied from conical forms to discoidal forms. Bivalve and gastropods are common (*ca*. 5%). Echinoderms and small benthic foraminifers are minor (less than 3%).

Interpretation: The diversified fauna suggests an open marine environment. The presence of green algae and gastropods indicates shallow water conditions (Flügel, 2010). Considering its stratigraphic relationship with MF6, MF7 was deposited in a shallow subtidal environment.

MF8 Green algae wackestone

Description: Strata with green algae (10–30%) set in micritic matrix occur at the upper part of the Xiongba section (Fig. 2H). Most of the green algae are dasyclads and are well preserved. Abundant peloids are present, along with minor conical orbitolinids and small benthic foraminifers, while echinoderms occur rarely.

Interpretation: Dasyclads thrive in water depths of no more than 10 meters (Banner & Simmons, 1994). The presence of peloids and micrite is typical of lagoonal environments (Flügel, 2010). Additionally, the shape of orbitolinids indicates shallower water conditions. Therefore, MF8 was deposited in a shallow lagoon.

Discussion

Palaeoenvironmental interpretations of strata enriched in discoidal orbitolinids

The mid-Cretaceous stratigraphic levels rich in discoidal orbitolinids have been observed in many locations, such as Middle East (Rahiminejad & Hassani, 2016; Xu *et al*., 2023), western Tethys (Di Lucia *et al*., 2012) and the North Atlantic (Douglass, 1960). The palaeoenvironmental interpretations of the orbitolinid-rich level have been debated (Di Lucia *et al*., 2012; Rahiminejad & Hassani, 2016). As previous studies have linked the morphology of orbitolinid tests to water depth, discoidal orbitolinids are often related to deeper environments (Banner & Simmons, 1994; Vilas *et al*., 1995; Rahiminejad & Hassani, 2016). However, it has been suggested that the water turbidity may also control their morphology; *i.e*., the flat forms often occurred in marlstone could be the results of turbid water rather than deep water (Pittet *et al*., 2002).

However, several pieces of evidence suggest that discoidal orbitolinids of the Xiongba section were inhabited in relatively deeper water. First, the biota of MF1 and MF2 include discoidal orbitolinids, echinoderms, bivalves, and sponge spicules; all these organisms, except for discoidal orbitolinids, represent a typical heterotrophic association. Such associations are common in deeper waters of tropical regions or in cooler waters at higher latitudes (Halfar *et al*., 2004). In contrast, MF5, MF6 and MF7 are characterized by abundant green algae besides the conical orbitolinids, indicating a warm and euphotic zone. Considering the palaeolatitude of the northern Lhasa terrane situated at *ca*. 15–20° N (Ma *et al*., 2018; Bian *et al*., 2020), it indicates that the palaeodepth of discoidal orbitolinids must be greater than that of conical orbitolinids. Additionally, diversified small benthic foraminifers co-occur only with conical orbitolinids, further implying shallower water depths for the latter.

Palaeoenvironmental changes of the Langshan Formation in the Xiongba section

The lower part of the Langshan Formation in the Xiongba section (0–140 m) is dominated by MF1, indicating relatively deep subtidal environments (Fig. 3). Occasional high-energy events increase the abundance of flat orbitolinids, resulting in the occurrence of discoidal orbitolinid packstone (Fig. 3). Between 140 and 160 m, the most prevalent lithofacies consists of small benthic foraminifer-conical orbitolinid wackestone and sponge spicule wackestone, indicating shallow subtidal environments (Fig. 3). The upper part of the Xiongba section (160–293 m) is mainly featured by an alternation of small benthic foraminifer-conical orbitolinid wackestone, orbitolinid-green algae wackestone to packstone, and green algae wackestone, all suggesting a lagoonal environment (Fig. 3). Therefore, the Langshan Formation in the Xiongba section represents an upward shallowing sequence from deep subtidal to shallow subtidal environments (Fig. 3).

In the Xiongba section, the Langshan Formation conformably overlies the Duoni Formation. The upper

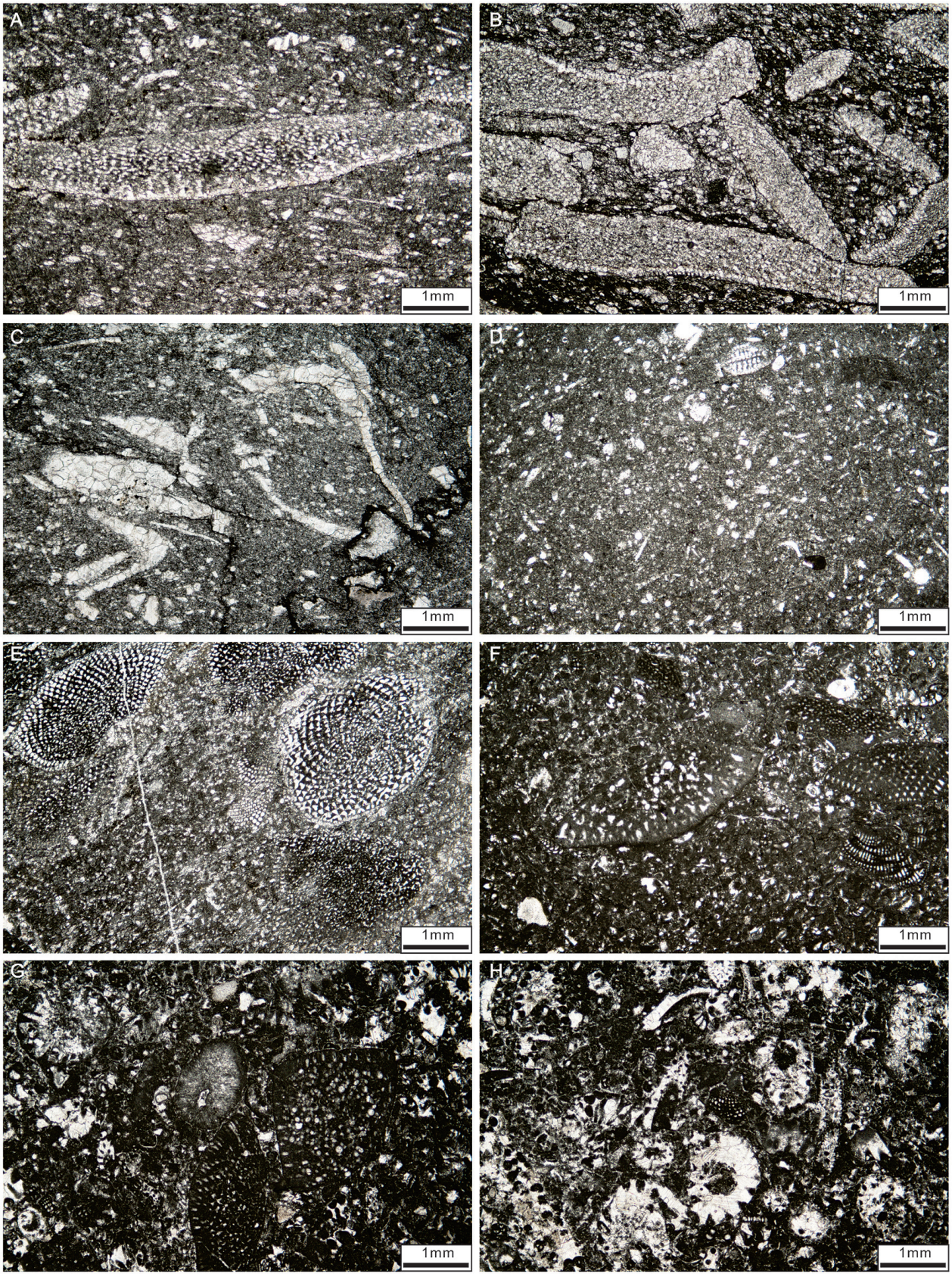

FIGURE 2. Microfacies of the Langshan Formation in the Xiongba section. **A**, MF1 Bioclast- discoidal orbitolinid wackestone. **B**, MF2 Discoidal orbitolinid packstone. **C**, MF3 Bivalve wackestone. **D**, MF4 Sponge spicule wackestone. **E**, MF5 Spicule-conical orbitolinid wackestone. **F**, MF6 Small benthic foraminifer-conical orbitolinid wackestone. **G**, MF7 Orbitolinid-green algae wackestone to packstone. **H**, MF8 Green algae wackestone.

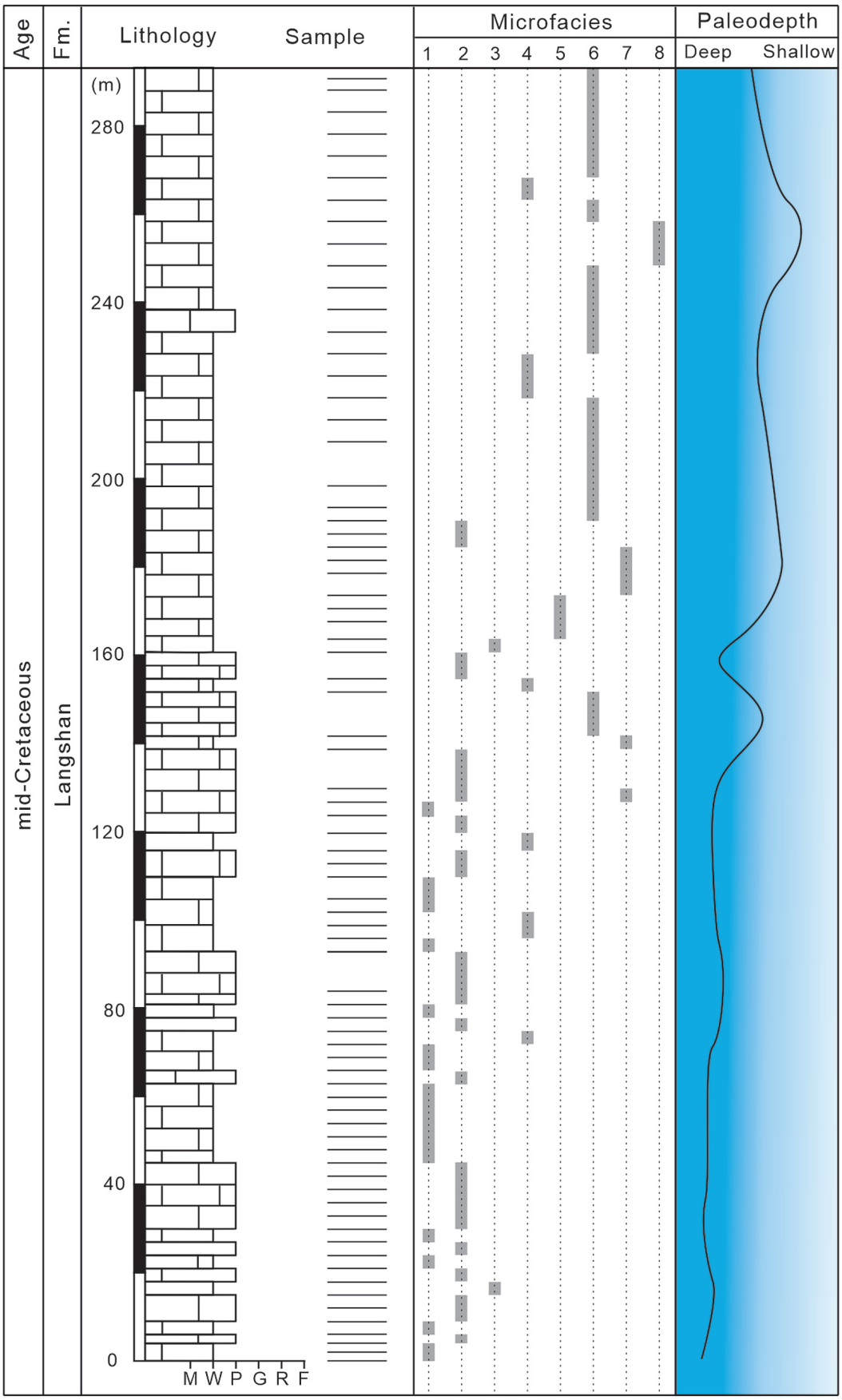

FIGURE 3. Stratigraphy of the Langshan Formation and microfacies distribution in the Xiongba section. See text for descriptions of microfacies MF1 to MF8.

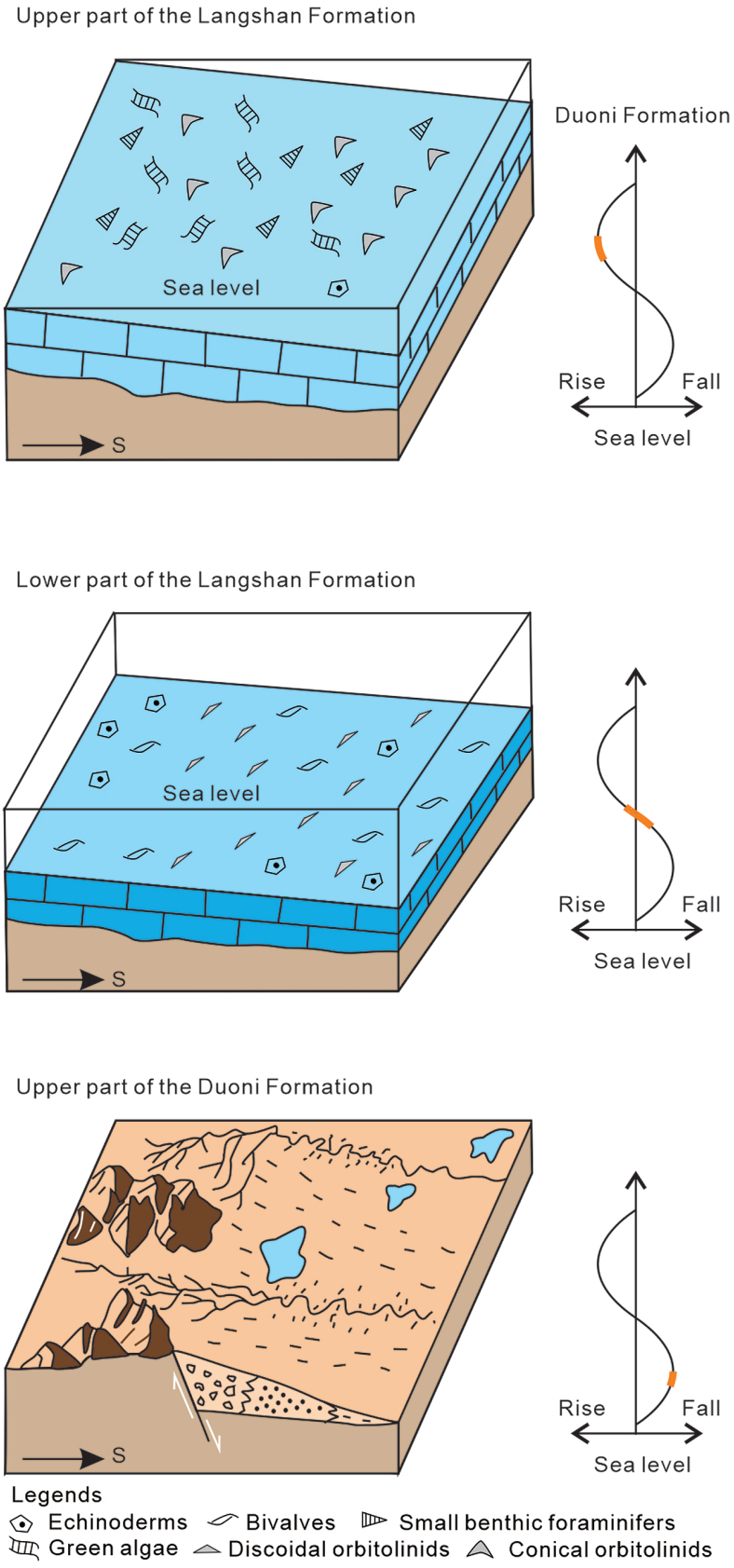

FIGURE 4. Mid-Cretaceous palaeogeographic evolution in Duba village. The depositional environment of the upper Duoni Formation was a fluvial floodplain, representing a lowstand in sea level. The boundary between the Duoni Formation and the Langshan Formation may represent a marine flooding surface, where discoidal orbitolinid limestone overlies the surface, indicating a dramatic deepening event. The discoidal orbitolinids were gradually replaced by conical orbitolinids and green algae, reflecting a normal regression during a period of slow sea-level rise.

part of the Duoni Formation was deposited in fluvial environments (Lai *et al*., 2019a) (Fig. 4). Thus, the transition from fluvial deposits to the marine limestone of the Langshan Formation represents a transgression that can be correlated across the entire northern Lhasa block (Xu *et al*., 2022). This transgression indicates a sudden flooding episode (Fig. 4), documented by the presence of deep subtidal discoidal orbitolinid levels subsequently followed by gradual depositional regression, culminating in conical orbitolinids and green algae (Fig. 4).

Conclusion.

In this study, microfacies analysis and palaeoenvironmental studies were carried out on the mid-Cretaceous limestone rich in orbitolinids from the Langshan Formation in the Duba village, central Tibet. Eight microfacies were identified, including bioclast-discoidal orbitolinid wackestone (MF1), discoidal orbitolinid packstone (MF2), and bivalve wackestone (MF3), which were deposited in relatively deep subtidal environments influenced by high-energy events. Additionally, sponge spicule wackestone (MF4), spicule-conical orbitolinid wackestone (MF5), and small benthic foraminifer-conical orbitolinid wackestone (MF6) were deposited in shallow subtidal environments, while orbitolinid-green algae wackestone to packstone (MF7) and green algae wackestone (MF8) were formed in lagoonal settings. The palaeoenvironmental reconstruction of the Langshan Formation reveals a general shallowing upward sequence. The lower part of the Xiongba section, characterized by discoidal orbitolinid limestones, was formed during a rapid transgression, whereas its upper part, represented by conical orbitolinid limestones with green algae, was deposited during a normal regression phase.

Acknowledgments

This paper is dedicated to Li Juan, who left us in her fieldwork in Tibet. This study was financially supported by the Fundamental Research Funds for NIGPAS (NGBS202405), the National Natural Science Foundation of Jiangsu Province (BK20242112), National Natural Science Foundation of China (42202118) and the Second Tibetan Plateau Scientific Expedition and Research Program (STEP, Grant No. 2019QZKK0204).

References

Banner, F.T. & Simmons, M.D. (1994) Calcareous algae and foraminifera as water-depth indicators: an example from the Early Cretaceous carbonates of northeast Arabia. In: Simmons, M.D., (Eds), *Micropalaeontology and Hydrocarbon Exploration in the Middle East: British Micropalaeontological Society Publications Series*, 243–252.

Bian, W., Yang, T., Jiang, Z., Jin, J., Gao, F., Wang, S. & Deng, C. (2020) Paleomagnetism of the Late Cretaceous red beds from the far western Lhasa terrane: Inclination discrepancy and tectonic implications. *Tectonics*, 39 (8), e2020TC006280. https://doi.org/10.1029/2020TC006280

BouDagher-Fadel, M.K., Hu, X.M., Price, G.D., Sun, G.Y., Wang, J.G. & An, W. (2017) Foraminiferal biostratigraphy and palaeoenvironmental analysis of the Mid-Cretaceous limestones in the southern Tibetan Plateau. *Journal of Foraminiferal Research*, 47 (2), 188–207. https://doi.org/10.2113/gsjfr.47.2.188.

Davies, R.B., Casey, D.M., Horbury, A.D., Sharland, P.R. & Simmons, M.D. (2002) Early to mid-Cretaceous mixed carbonate-clastic shelfal systems: examples, issues and models from the Arabian Plate. *GeoArabia*, 7 (3), 541–598. https://doi.org/10.2113/geoarabia0703541

Dewey, J.F., Shackleton, R.M., Chang, C.F. & Sun, Y.Y. (1988) The tectonic evolution of the Tibetan Plateau. *Royal Society of London Philosophical Transactions, ser. A: Mathematical and Physical Sciences*, 327, 379–413. https://doi.org/10.1098/rsta.1988.0135

Di Lucia, M., Trecalli, A., Mutti, M. & Parente, M. (2012) Bio-chemostratigraphy of the Barremian-Aptian shallow-water carbonates of the southern Apennines (Italy): pinpointing the OAE1a in a Tethyan carbonate platform. *Solid Earth*, 3 (1), 1–28. https://doi.org/10.5194/se-3-1-2012

Douglass, R.C. (1960) *The Foraminiferal Genus Orbitolina in North America: A Study of the Genus Orbitolina, Its Type Species, Morphology, and Stratigraphic and Geographic Distribution in North America (Vol. 333)*. US Government Printing Office, 52 pp. https://doi.org/10.3133/pp333

Dunham, R.J. (1962) Classification of carbonate rocks according to depositional textures. *In*: Ham, W.E. (Ed.), *Classification of Carbonate Rocks. American Association of Petroleum Geologists Memoir*, 1, 108–121. https://doi.org/10.1306/M1357

Fan, J.J., Li, C., Xie, C.M. & Wang, M. (2014) Petrology, geochemistry, and geochronology of the Zhonggang ocean island, northern Tibet: implications for the evolution of the Banggongco-Nujiang oceanic arm of the Neo-Tethys. *International Geology Review*, 56 (12), 1504–1520. https://doi.org/10.1080/00206814.2014.947639

Flügel, E. (2010) *Microfacies of carbonate rocks: Analysis, interpretation and application (2nd ed.)*. Springer-Verlag, Berlin, 924 pp. https://doi.org/10.1007/978-3-642-03796-2.

Halfar, J., Godinez-Orta, L., Mutti, M., Valdez-Holguín, J.E. & Borges, J.M. (2004) Nutrient and temperature controls on modern carbonate production: an example from the Gulf of California, Mexico. *Geology*, 32 (3), 213–216. https://doi.org/10.1130/G20298.1

Hu, X., Ma, A., Xue, W., Garzanti, E., Cao, Y., Li, S., Sun, G. & Lai, W. (2022) Exploring a lost ocean in the Tibetan Plateau: Birth, growth, and demise of the Bangong-Nujiang Ocean. *Earth-Science Reviews*, 229, 104031. https://doi.org/10.1016/j.earscirev.2022.104031

James, N.P. & Jones, B. (2015) *Origin of carbonate sedimentary rocks*. John Wiley & Sons, 464 pp.

Kapp, P., DeCelles, P.G., Gehrels, G.E., Heizler, M. & Ding, L. (2007) Geological records of the LhasaQiangtang and Indo-Asian collisions in the Nima area of central Tibet. *Geological Society of America Bulletin*, 119, 917–933. https://doi.org/10.1130/B26033.1

Kapp, P. & DeCelles, P.G. (2019) Mesozoic–Cenozoic geological evolution of the Himalayan-Tibetan orogen and working tectonic hypotheses. *American Journal of Science*, 319 (3), 159–254. https://doi.org/10.2475/03.2019.01

Lai, W., Hu, X., Garzanti, E., Xu, Y., Ma, A. & Li, W. (2019a) Early Cretaceous sedimentary evolution of the northern Lhasa terrane and the timing of initial Lhasa-Qiangtang collision. *Gondwana Research*, 73, 136–152. https://doi.org/10.1016/j.gr.2019.03.016

Lai, W., Hu, X., Garzanti, E., Sun, G., Garzione, C.N., Fadel, M.B. & Ma, A. (2019b) Initial growth of the northern Lhasaplano, Tibetan Plateau in the early Late Cretaceous (ca. 92 Ma). *Geological Society of America Bulletin*, 131, 1823–1836. https://doi.org/10.1130/B35124.1

Leeder, M.R., Smith, A.B. & Jixiang, Y. (1988) Sedimentology, palaeoecology and palaeoenvironmental evolution of the 1985 Lhasa to Golmud Geotraverse. *Royal Society of London Philosophical Transactions, ser. A: Mathematical and Physical Sciences*, 327, 107–143. https://doi.org/10.1098/rsta.1988.0123

Leier, A.L., DeCelles, P.G., Kapp, P. & Gehrels, G.E. (2007) Lower Cretaceous strata in the Lhasa Terrane, Tibet, with implications for understanding the early tectonic history of the Tibetan Plateau. *Journal of Sedimentary Research*, 77, 809–825. https://doi.org/10.2110/jsr.2007.078.

Li, S., Yin, C., Guilmette, C., Ding, L. & Zhang, J. (2019) Birth and demise of the Bangong-Nujiang Tethyan Ocean: A review from the Gerze area of central Tibet. *Earth-Science Reviews*, 198, 102907. https://doi.org/10.1016/j.earscirev.2019.102907

Ma, A.L., Hu, X.M., Garzanti, E., Han, Z. & Lai, W. (2017) Sedimentary and tectonic evolution of the southern Qiangtang basin: Implications for the Lhasa-Qiangtang collision timing. *Journal of Geophysical Research: Solid Earth*, 122, 4790–4813. https://doi.org/10.1002/2017JB014211

Ma, Y., Yang, T., Bian, W., Jin, J., Wang, Q., Zhang, S. & Cao, L. (2018) A stable southern margin of Asia during the Cretaceous: Paleomagnetic constraints on the Lhasa-Qiangtang collision and the maximum width of the Neo-Tethys. *Tectonics*, 37 (10), 3853–3876. https://doi.org/10.1029/2018TC005143

Pan, G.T., Ding, J., Yao, D.S. & Wang, L.Q. (2004) *Guide Book of 1:1,500,000 Geologic Map of the QinghaiXizang (Tibet) Plateau and Adjacent Areas*. Cartographic Publishing House, Chengdu,148 pp.

Pittet, B., Van Buchem, F.S.P., Hillgärtner, H., Razin, P., Grötsch, J. & Droste, H. (2002) Ecological succession, palaeoenvironmental change, and depositional sequences of Barremian–Aptian shallow-water carbonates in northern Oman. *Sedimentology*, 49, 555–581. https://doi.org/10.1046/j.1365-3091.2002.00460.x

Rao, X., Skelton, P.W., Sha, J., Cai, H. & Iba, Y. (2015) Mid-Cretaceous rudists (Bivalvia: Hippuritida) from the Langshan Formation, Lhasa block, Tibet. *Papers in Palaeontology*, 1, 401–424. https://doi.org/10.1002/spp2.1019

Rahiminejad, A.H. & Hassani, M.J. (2016) Paleoenvironmental distribution patterns of orbitolinids in the Lower Cretaceous deposits of eastern Rafsanjan, Central Iran. *Marine Micropaleontology*, 122, 53–66. https://doi.org/10.1016/j.marmicro.2015.11.006

Sun, G., Hu, X., Sinclair, H.D., BouDagher-Fadel, M.K. & Wang, J. (2015) Late Cretaceous evolution of the Coqen Basin (Lhasa terrane) and implications for early topographic growth on the Tibetan Plateau. *Geological Society of America Bulletin*, 127, 1001–1020. https://doi.org/10.1130/B31137.1

Sun, G., Hu, X. & Sinclair, H.D. (2017) Early cretaceous palaeogeographic evolution of the Coqen basin in the Lhasa Terrane, southern Tibetan plateau. *Palaeogeography, Palaeoclimatology, Palaeoecology*, 485, 101–118. https://doi.org/10.1016/j.palaeo.2017.06.006

Vilas, L., Masse, J.P. & Arias, C. (1995) Orbitolina episodes in carbonate platform evolution: the early Aptian model from SE Spain. *Palaeogeography, Palaeoclimatology, Palaeoecology*, 119 (1-2), 35–45. https://doi.org/10.1016/0031-0182(95)00058-5

Wilson, J.L. (1975) *Carbonate facies in geologic history*. Springer Science & Business Media, 471 pp. https://doi.org/10.1007/978-1-4612-6383-8

Xu, Y., Hu, X., BouDagher-Fadel, M.K., Sun, G., Lai, W., Li, J. & Zhang, S. (2020) The major Late Albian transgressive event recorded in the epeiric platform of the Langshan Formation in central Tibet. *In*: Wagreich, M., Hart, M.B., Sames, B. & Yilmaz, I.O. (Eds), Cretaceous Climate Events and Short-Term Sea Level Changes. *Geological Society, London, Special Publication*, 498, 211–232. https://doi.org/10.1144/SP498-2019-8.

Xu, Y., Hu, X., Garzanti, E., BouDagher-Fadel, M., Sun, G., Lai, W. & Zhang, S. (2022) Mid-Cretaceous thick carbonate accumulation in Northern Lhasa (Tibet): eustatic vs. tectonic control?. *Geological Society of America Bulletin*, 134 (1-2), 389–404.
https://doi.org/10.1130/B35930.1

Xu, Y., Hu, X., Garzanti, E., Sun, G., Jiang, J., Li, J. & Rao, X. (2023) Carbonate factories and their critical control on the geometry of carbonate platforms (mid-Cretaceous, southern Iran). *Palaeogeography, Palaeoclimatology, Palaeoecology*, 625, 111680.
https://doi.org/10.1016/j.palaeo.2023.111680

Yin, A. & Harrison, T.M. (2000) Geologic evolution of the Himalayan-Tibetan orogen. *Annual Review of Earth and Planetary Sciences*, 28, 211–280.
https://doi.org/10.1146/annurev.earth.28.1.211

Zhang, K.J., Xia, B.D., Wang, G.M., Li, Y.T. & Ye, H.F. (2004) Early Cretaceous stratigraphy, depositional environments, sandstone provenance, and tectonic setting of central Tibet, western China. *Geological Society of America Bulletin*, 116, 1202–1222.
https://doi.org/10.1130/B25388.1

Zhang, Q.H., Ding, L., Cai, F.L., Xu, X.X., Zhang, L.Y., Xu, Q. & Willems, H. (2011) Early Cretaceous Gangdese retroarc foreland basin evolution in the Selin Co basin, central Tibet: evidence from sedimentology and detrital zircon geochronology. *In*: Gloaguen, R. & Ratschbacher, L. (Eds), Growth and Collapse of the Tibetan Plateau. *Geological Society, London, Special Publication*, 353, 27–44.
https://doi.org/10.1144/SP353.3

Zhu, D.C., Li, S.M., Cawood, P.A., Wang, Q., Zhao, Z.D., Liu, S.A. & Wang, L.Q. (2016) Assembly of the Lhasa and Qiangtang terranes in central Tibet by divergent double subduction. *Lithos*, 245, 7–17.
https://doi.org/10.1016/j.lithos.2015.06.023

Zhu, Z., Zhai, Q., Hu, P., Tang, Y., Wang, H., Wang, W. & Wu, H. (2022) Resolving the timing of Lhasa-Qiangtang block collision: Evidence from the Lower Cretaceous Duoni Formation in the Baingoin foreland basin. *Palaeogeography, Palaeoclimatology, Palaeoecology*, 595.
https://doi.org/10.1016/j.palaeo.2022.110956